Analytica Chimica Acta 770 (2013) 153–160

Contents lists available at SciVerse ScienceDirect

Analytica Chimica Acta

journal homepage: www.elsevier.com/locate/aca

Disposable biosensor based on cathodic electrochemiluminescence of tris(2,2-bipyridine)ruthenium(II) for uric acid determination

J. Ballesta-Claver, R. Rodríguez-Gómez, L.F. Capitán-Vallvey*

ECsens, Department of Analytical Chemistry, Campus Fuentenueva, Faculty of Sciences, University of Granada, E-18071 Granada, Spain

HIGHLIGHTS

- Cathodic ECL offers conventional and non-aggressive analysis conditions.
- The ECL hydrogen peroxide/ruthenium complex system for uric acid determination is novel.
- The ruthenium complex is electrochemically immobilized on graphite screen-printed electrodes.
- The quantification of the uric acid is based on a Stern–Volmer type equation.
- The use of the cathodic ECL working methodology reduces interferences during analysis.

GRAPHICAL ABSTRACT

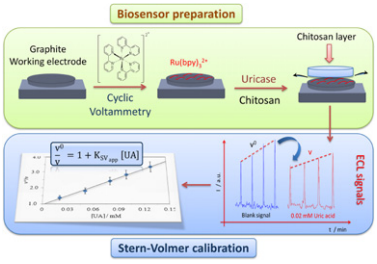

ARTICLE INFO

Article history:
Received 27 November 2012
Received in revised form 19 January 2013
Accepted 22 January 2013
Available online 1 February 2013

Keywords:
Cathodic electrochemiluminescence
Disposable biosensor
Immobilized $Ru(bpy)_3^{2+}$
Uric acid determination

ABSTRACT

A new method for uric acid (UA) determination based on the quenching of the cathodic ECL of the tris(2,2-bipyridine)ruthenium(II)–uricase system is described. The biosensor is based on a double-layer design containing first tris(2,2-bipyridine)ruthenium(II) ($Ru(bpy)_3^{2+}$) electrochemically immobilized on graphite screen-printed cells and uricase in chitosan as a second layer. The uric acid biosensing is based on the ECL quenching produced by uric acid over the cathodic ECL caused by immobilized $Ru(bpy)_3^{2+}$ in the presence of uricase. The use of a −1.1 V pulse for 1 s with a dwelling time of 10 s makes it possible to estimate the initial enzymatic rate, which is used as the analytical signal. The Stern–Volmer type calibration function shows a dynamic range from 1.0×10^{-5} to 1.0×10^{-3} M with a limit of detection of 3.1×10^{-6} M and an accuracy of 13.6% (1.0×10^{-4} M, $n = 5$) as relative standard deviation. Satisfactory results were obtained for urine samples, creating an affordable alternative for uric acid determination.

1. Introduction

The determination of uric acid in biological fluids such as urine and blood serum is a routine determination in clinical analysis and it is known that many disorders are directly related with variations in uric acid concentration [1–3]. Typically, the urinary excretion is between 1.49 and 4.46 mM (25–74 mg dL^{-1}) [4]. Uric acid (UA) can be analyzed by means of different techniques [5], but the use of electrochemiluminescence (ECL) can offer a new approach to analysis. ECL offers low detection limits and good sensitivity. For the analysis of uric acid by ECL, the usual luminophores are luminol [6,7] and oxalate derivatives [8]. These determinations are based on the enzymatic production of H_2O_2 by uricase which is oxidized, along with luminophore, in the working electrode producing an ECL signal that enhances with the uric acid concentration.

Another way to determine uric acid using ECL exists, which consists of the use of $Ru(bpy)_3^{2+}$ as luminophore. In this case, the determination of uric acid is based either on the inhibition of the $Ru(bpy)_3^{2+}$ blank ECL signal [3,9] or on the inhibition of the ECL emission of $Ru(bpy)_3^{2+}$-tripropylamine chemistry in the presence

* Corresponding author. Tel.: +34 958 248 436; fax: +34 958 243 328.
E-mail address: lcapitan@ugr.es (L.F. Capitán-Vallvey).

0003-2670/$ – see front matter © 2013 Elsevier B.V. All rights reserved.
http://dx.doi.org/10.1016/j.aca.2013.01.045

of a fluoro-surfactant modified gold electrode [10]. The use of $Ru(bpy)_3^{2+}$ has some advantages: it is not consumed, has good reproducibility and a higher ECL emission than luminol or oxalate derivatives. The immobilization of the $Ru(bpy)_3^{2+}$ complex for a biosensor preparation has received considerable attention and a great number of procedures have been used to their immobilization on solid surfaces, such as cationic ion-exchange, ion association, entrapment in sol–gel and other materials, electrostatic attachment, covalent bond, and layer-by-layer self-assembly [11]. Most of these immobilization procedures require the use of additional polymers or previous derivatization of the complex. In this work we use a simple electrochemical method to immobilize the complex.

On the other hand, cathodic ECL is a current trend and recently has included the use of other luminophores such as luminol [12,13], $Ru(bpy)_3^{2+}$ and nanomaterials like quantum dots (CdS, CdSe, CdTe and ZnS) [14]. The most suitable co-reactant used is peroxodisulfate anion ($S_2O_8^{2-}$) because of its capacity to form strong oxidant agents upon electrochemical reduction [15].

The use of the cathodic ECL or reductive–oxidative methods can have many different advantages, being a methodology with good perspectives in future because supposes an improvement in analytical determinations offering characteristics such as extending the number of possible ECL reactions, an eliminating the oxidation products of luminophores that reduce the functionality of the biosensor and even removing the interference of compounds present in the sample that could be oxidized on the electrode. It is not very widespread, due to the need for high reduction conditions, metal surfaces and organic solvents to carry it out [16]. In 2005, Bard et al. reported in an extensive preliminary study [17] that is possible to use $Ru(bpy)_3^{2+}$ as luminophore and H_2O_2 as the co-reactant using the reductive–oxidative reaction in aqueous medium. In this case, both H_2O_2 and ruthenium complex are reduced obtaining an intense ECL emission. This possibility of using ruthenium complexes with H_2O_2 as co-reactant paved the way to new ECL biosensing designs, probably because cathodic ECL can finally be extensively applied with all of its potential advantages.

The aim of this work is to develop a disposable biosensor for UA based on the quenching of the cathodic ECL of immobilized $Ru(bpy)_3^{2+}$ on graphite SPE cells. To the best of our knowledge, the use of cathodic ECL for uric acid biosensing based on H_2O_2 enzymatically has not been reported, constituting a basis for new ECL biosensors developing. We believe that it is possible to prepare disposable analytical devices to be included in portable instrumentation with the advantages of a short analysis time and the elimination of common interferences [18].

2. Experimental

2.1. Chemicals

Saline buffers were prepared in 0.625 M NaCl as electrolyte with 0.6 M Tris (99% Trizma base) and 0.6 M phosphate (Na_2HPO_4), adjusted to different pHs by adding NaOH or HCl. Stock solutions of 10^{-3} M uric acid (UA), prepared by weighing uric acid directly (Sigma–Aldrich Química S.A., Madrid, Spain), and 0.01 mM solutions of ascorbic acid and urea (Sigma) were used. A 10^{-4} M solution of tris(2,2′-bipyridyl)dichloro ruthenium(II) ($Ru(bpy)_3^{2+}$) was prepared from its hexahydrate in 0.1 M KNO_3. Uricase from *Bacillus fastidiosus* (5 mg, 14.5 U mg^{-1}) was prepared with 5 mg and 1 mL of 0.1 M Tris buffer pH 8.5 in an Eppendorf tube and shaken for 2 min, then aliquoted and preserved at −20 °C until use [19]. Chitosan was prepared by dissolving 1 g in 100 mL water, containing 1 mL of acetic acid (95.5%, Panreac, Barcelona, Spain) by shaking for 4 h. Reverse-osmosis type quality water (Milli-Q Plus185 from Millipore, Molsheim, France) was used throughout.

Graphite screen-printed electrodes (SPE) and gold nanoparticle-modified screen-printed carbon electrodes (GNP-SPCE) were supplied by Dropsens (Oviedo, Spain). These electrochemical cells consist of a round working electrode 4 mm in diameter, a counter electrode, both with the same material, and a silver pseudo-reference electrode on a ceramic support. Before being used, the electrochemical cells were tested for uniform behavior. In order to prepare a receptacle on the disposable electrochemical cell, the electrode area was covered with successive layers of plastic white adhesive tape up to 1 mm thick with an 8 mm diameter hole (50 μL volume) in the sensing area. Before using the SPE cells, pretreatment was performed by immersing the electrochemical cells in 0.2 M H_2SO_4 and applying three voltammetric sweeps between −0.2 and 1.0 V. After that, the SPE cells were dried for 10 min at room temperature.

2.2. Apparatus and software

The ECL emissions from the SPE were measured using a H8529 photomultiplier (PMT) interfaced to a C8855 USB photo counting unit, both from Hamamatsu (Hamamatsu Technologies K.K., Shizuoka, Japan). The potentiostat Autolab PGSTAT 128N with F120 module for cronocoulometric measurements with NOVA 1.8 software (Metrohm Autolab B.V., Utrecht, The Netherlands) including a connector for screen-printed electrodes supplied by Dropsens was used. The arrangement used for ECL studies was described previously [20] and basically consists of a black box that contains two black methacrylate piece holders, which fit one on top of the other, one to insert the electrochemical cell in a fixed position and the other containing the PMT. Other instruments consist of a Crison digital pH-meter (Crison Instruments, Barcelona, Spain) with combined glass-saturated calomel electrode. Additionally, a variable pressure scanning electron microscopy LEO 1430-VP (VPSEM) was used for imaging increases ranging from 15× to 300k×, and a ZEISS DSM 250 electron microscope prepared to perform energy dispersive X-ray spectroscopy (EDX) microanalysis. For the in situ-FTIR measurements, a Nicolet Magna IR-spectrometer using a liquid nitrogen-cooled MCT detector was employed. A Roche Hitachi-912 enzymatic auto-analyzer (Hitachi High-Technologies Europe, Germany) was used as a reference method for uric acid in 24 h-urine samples.

2.3. Biosensor preparation

A pre-treatment of graphite screen-printed cells is necessary to remove organic ink constituents and/or contaminants, increasing surface roughness and the graphite functionalities. Then, five sweeps were carried out from 0.0 to 2.1 V at 0.1 V s^{-1} in a 0.1 M KNO_3.

The UA biosensor was prepared by immersing the SPE cells in 10^{-4} M $Ru(bpy)_3^{2+}$ containing 0.1 M KNO_3, bubbling N_2 for 15 min before immobilizing the ruthenium complex, and cycling from 0.0 to 2.1 V at 0.2 V s^{-1}, with 60 cycles. Then, 4 μL of the chitosan–uricase mixture (1:4 ratio) was dropped on the working electrode before waiting about 1 h for it to dry at room temperature. The biosensor was washed with 0.2 M phosphate buffer pH 9.0 in order to make sure that no ruthenium complex and enzyme traces remained. After that, the electrochemical cells were stored in dark conditions at 4 °C until use.

2.4. ECL analytical signal

After applying a set of four consecutive pulses of −1.1 V for 1 s with a dwelling time of 10 s on graphite SPE cells, the analytical signal was obtained as the slope, in mV s^{-1}, of the four first pulses.

2.5. Procedures

2.5.1. Standards

Volumes of 50 μL of different UA standards prepared from 10^{-3} M UA stock solution in 0.2 M pH 9.0 phosphate buffer containing 0.25 M NaCl were dropped on the SPE cell receptacle. The uric acid-sensitive biosensor was placed in the black holder and covered with the lid holding the PMT, obtaining the ECL analytical signal as indicated above.

2.5.2. Urine samples

A 24 h-urine sample was diluted 100-fold with 0.2 M phosphate buffer pH 9.0 and NaCl 0.25 M. After that, 50 μL was placed in the receptacle of the SPE cells working as previously described.

3. Results and discussion

Uric acid, like some amino acids, seriously interferes in the ECL emission of some luminophores such as $Ru(bpy)_3^{2+}$, even at low concentrations [21]. This is the basis of conventional ECL procedures for UA through the inhibition of the ECL emission [9,21]. However, the use of $Ru(bpy)_3^{2+}$ complex as luminophore by using a cathodic ECL supposes an advantage in enzymatic determinations. The immobilization procedure of reagents is key for good biosensor responses. In this paper we immobilized ruthenium complex on a screen-printed carbon electrode by an electrochemical method that results in a composite that offers the advantages of better conductivity and accessibility.

3.1. Biosensor structure

3.1.1. Immobilization of $Ru(bpy)_3^{2+}$

The immobilization by electropolymerization requires monomers that contain polymerizable groups in their molecules but, in our case, the $Ru(bpy)_3^{2+}$ complex does not contain this kind of group. However, Premkumar and Khoo [22] have demonstrated that it is possible to immobilize it on a glassy carbon conventional electrode surface by a potentiodynamic technique obtaining a glassy carbon oxide (GCO)/$Ru(bpy)_3^{2+}$ composite film. In this paper, we study the possibility of the immobilization of the Ru complex on graphite SPE cells in a different way.

A cyclic voltammetry (from 0.0 to 2.1 V at 0.2 V s^{-1}) of a deaerated solution containing 10^{-4} M $Ru(bpy)_3^{2+}$ and 0.1 M KNO_3 in a graphite SPE cell produce an immobilization of the complex. The immobilization was checked measuring the ECL emission produced by a 10^{-6} M H_2O_2 solution in the electrochemical cell after washing.

The redox peaks of the ruthenium complex in solution appear around 1.3 V using an Ag/AgCl reference electrode with conventional electrodes, but on graphite SPE cells, a reduction peak is observed near 1.0 V which grows with each cycle (Fig. 1A). This data agree with the results from Premkumar and Khoo [22] with respect to the shift to less positive potentials, which is indicative of the immobilization of the $Ru(bpy)_3^{2+}$ complex on the electrode.

Furthermore, the oxidation peak of immobilized $Ru(bpy)_3^{2+}$ is not observed in Fig. 1A, as a continuous oxidation process occurs between 1.2 V and 2.1 V, which has been attributed to the oxidation of the graphite [23], in our case from both electrodes, the SPE working and counter electrodes.

For a deeper understanding of the immobilization process, we substituted the reference and counter electrodes of the SPE cell with external hydrogen reference electrode, using a lugging probe capillary, and platinum counter electrode, observing that several new oxidation and reduction peaks appeared (Fig. 1B). The two groups of observed peaks at (E_{ox}/E_{red}) 1.43/1.39 V, 1.62/1.58 V are right shifted because we used a different reference electrode (SHE instead of Ag/AgCl), which gradually increase during cycling, can be ascribed to an activation of the graphite surface producing oxidized films containing quinone-like groups and carboxylic functionalities [23] that could enable the attachment of the ruthenium complex. The peaks observed at E_{ox} 1.7 V and E_{red} 1.65 V are ascribed to the complex in solution.

The electrochemical characterization of the SPE cell was carried out using external electrodes and immersing the previously prepared SPE cell with the immobilized ruthenium complex in a 0.1 M KNO_3 solution. Cycling from 0.2 to 1.5 V in this solution, the presence of the immobilized ruthenium complex (E_{ox}/E_{red}, 1.40/1.32) is revealed along with the corresponding peaks of the oxidized forms of graphite (Fig. 1C). Additionally, this figure shows that successive cycles produce a leaching of the luminophore, indicating a slight retention.

A spectroscopic study of the modification of the graphite surface has been done. First, an infrared study revealed the immobilization of the ruthenium complex on the graphite surface. The total reflectance spectra (ATR) of $Ru(bpy)_3^{2+}$ electrochemically immobilized on a conventional electrode of graphite (Fig. 1D) show similar bands to the spectrum of solid $Ru(bpy)_3^{2+}$ in KBr. The triplet observed between 1400 and 1500 cm^{-1} in the ATR spectrum can be ascribed to 2,2′-bipyridine groups (δ C—CH; ν C—C; ν C—N) [24], indicating the presence of the ruthenium complex in the graphite electrode. Additionally, the ruthenium complex has an attenuated band around 1600 cm^{-1} (Fig. 1D-1), but in the ATR spectrum (Fig. 1D-2), this band increased due to the formation of carbonyl groups on the surface of the graphite bar that hides the ruthenium complex band [25].

Secondly, the immobilization of $Ru(bpy)_3^{2+}$ on the SPE cell was confirmed by SEM and EDX. These studies were carried out on Au metalized graphite electrochemical cells (GNP-SPCE). Fig. 2 shows a rough surface on the treated electrode where the ruthenium complex is included, as the EDX spectrum confirms (Fig. 2C).

3.1.2. Recognition layer

In this case the immobilization of the enzyme must be done over the modified graphite SPE containing $Ru(bpy)_3^{2+}$. Additionally, the weak retention of the luminophore, as shown by the above indicated leaching, can be improved by including the enzyme in an upper layer. For that purpose, chitosan, an N-deacetylated polyelectrolyte derived from biopolymer chitin [26], was used with good results because the negatively charged uricase enzyme is electrostatically retained with the positively charged chitosan [27].

3.2. Sensing mechanism and analytical signal

The determination of uric acid presented in this paper is based on the quenching of the cathodic ECL of the $Ru(bpy)_3^{2+}$/uricase system.

It is known that $Ru(bpy)_3^{2+}$ in solution and in the presence of oxygen produces ECL by a reductive route, as Bard et al. reported [17], via H_2O_2 formation and consecutively reactive oxygen species (ROS) [28]. In this case, the addition of H_2O_2 strongly increases the ECL emission.

We observed that the $Ru(bpy)_3^{2+}$ complex immobilized on oxidized graphite SPE has a higher ECL signal when compared to the solution, some four times when working with the same amount of complex in solution and when is immobilized (Fig. 3a). This data agrees with the described ECL enhancing of $Ru(bpy)_3^{2+}$ when using an oxidized graphite conventional electrode [28].

The presence of uricase strongly increases the ECL signal of the immobilized $Ru(bpy)_3^{2+}$, both with the uricase in solution (20 times) and when immobilized in the polymer chitosan (13.6 times, Fig. 3c). The reason for the enhancement of the ECL emission may be the catalytic effect of metals present in the enzyme, such as copper or iron (the copper:uricase ratio was 1:7 and the iron:uricase

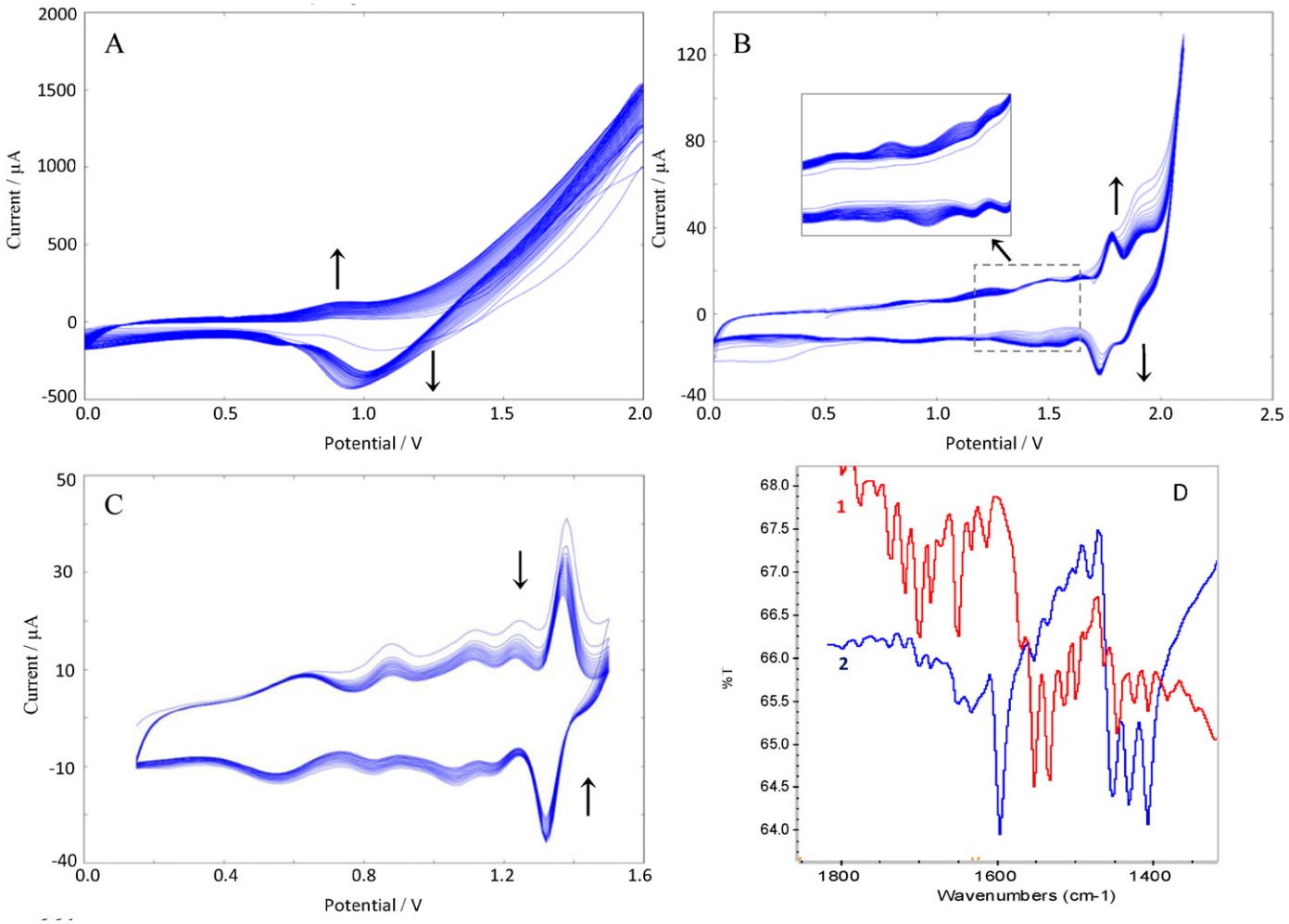

Fig. 1. Cyclic voltammetries of a $Ru(bpy)_3^{2+}$ 10^{-4} M and 0.1 M of KNO_3 solution under N_2 conditions. (A) Graphite SPE cell using its own pseudo-Ag reference; (B) graphite SPE cell using an external hydrogen reference electrode and platinum counter electrode. It is possible to see the oxidation of the graphite SPE surface (see the inset) and increased peaks at 1.7 V due to $Ru(bpy)_3^{2+}$ in solution; (C) a characterization study of the graphite SPE cell in KNO_3 0.1 M, 20 cycles and 10^{-4} M $Ru(bpy)_3^{2+}$, with an anodic limit of 2.1 V, shows the immobilization of the complex at 1.4 V and the presence of the carbon oxides; (D) ATR spectrum of $Ru(bpy)_3^{2+}$ immobilized on a graphite conventional electrode (1) and FTIR spectrum of $Ru(bpy)_3^{2+}$ in KBr pellet (2).

ratio was 1:50) [29,30], which agrees with the data reported by Qiu et al. [31] on $Ru(bpy)_3^{2+}$ ECL enhancement using metal ions, producing OH radicals. Additionally, it was observed that with the sole use of chitosan as the membrane polymer, the ECL signal increases (3.5 times), probably due to a reduction of the ruthenium complex leaching and an improvement in the inter-connection between the ruthenium complex molecules by the chitosan electroactive membrane (Fig. 3b).

In the presence of UA, the SPE biosensor triggers two different reactions. First, its oxidation catalyzed by uricase generates H_2O_2 which is electrochemically reduced at −0.41 V along with the $Ru(bpy)_3^{2+}$. Second, the scavenger role of UA, which eliminates the ROS coming from the H_2O_2, prevents the formation of any excited $Ru(bpy)_3^{2+*}$ species and quenches the ECL emission [32]. In short, the addition of UA dramatically reduces the ECL signal previously observed in diagram 1 and Fig. 3d.

The quenching behavior of the system can be described by the Stern–Volmer equation (Eq. (1)) where I^0 and I are the ECL signals in the absence and presence of the quencher, respectively.

$$\frac{I^0}{I} = 1 + K_{SV_{app}}[UA] \quad (1)$$

This $K_{SV_{app}}$ constant is an apparent Stern–Volmer constant because the observed quenching depends on UA quencher. Furthermore, using the analytical concentration of the UA present, it was observed that the K_{sv} constant varies between $(2.0 \pm 0.1) \times 10^4$ M at 190 s and $(2.4 \pm 0.1) \times 10^4$ M at 380 s, obtaining a Stern–Volmer constant that depends on acquisition time. The enzymatic production of H_2O_2 with time results in a little inhibition effect on the ECL over the sole inhibitory effect of UA [17] when the time is long. The mechanism is presented in Fig. 4 .

To calculate the analytical parameter for the quantification of uric acid we used the initial rate ($v = \Delta I/\Delta t$). The analytical parameter was the ratio of the initial rate for the blank and standard, respectively (v^0/v). The Stern–Volmer type equation changes as follows:

$$\frac{v^0}{v} = 1 + K_{SV_{app}}[UA] \quad (2)$$

3.3. Optimization of the uric acid biosensor

The preparation of the uric acid biosensor is influenced by different factors, such as the number of cyclic sweeps and the concentrations of enzyme and chitosan.

3.3.1. Cycle number

The cycle number used for Ru complex immobilization is a very important factor. The ECL intensity grows with cycling, that is,

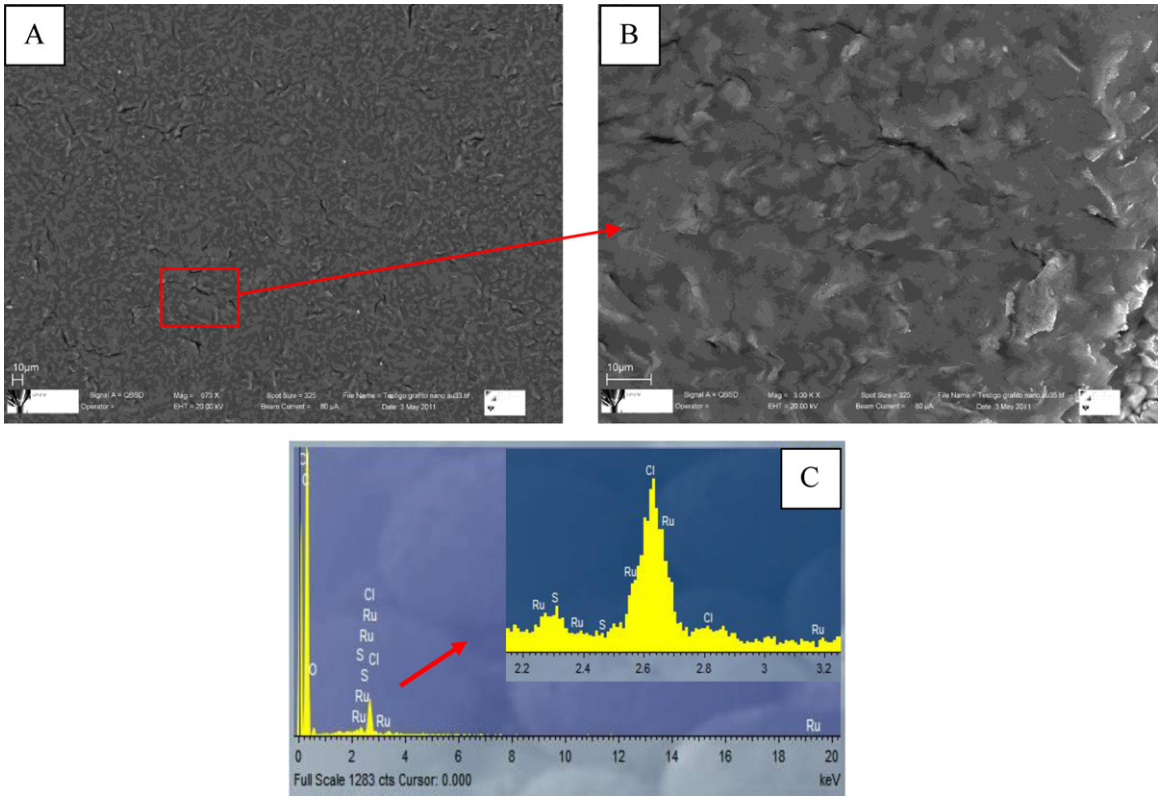

Fig. 2. SEM and EDX images on GNP-SPCE cell with attached $Ru(bpy)_3^{2+}$ (A and B); (C) EDX image shows the presence of ruthenium molecules on the working electrode.

the amount of $Ru(bpy)_3^{2+}$ immobilized, reaching a maximum at 60 cycles (Fig. 5A). The increase in the surface roughness of the graphite working electrode with cycling [33] probably facilitates the complex immobilization. The later reduction observed in the ECL at high cycle number agrees with the evolution of the net charge (net Q_+/Q_-) on the working electrode during the cyclic voltammetry (Fig. 5A), maybe due to the deterioration of the electrode surface, which reduces the amount of luminophore retained. At this point, 60 cycles was selected for the $Ru(bpy)_3^{2+}$ immobilization.

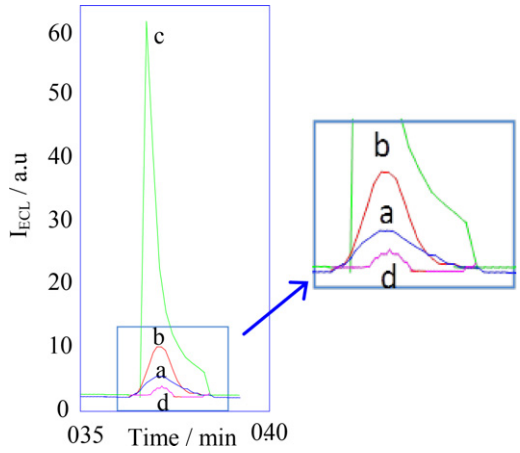

Fig. 3. Effect of the addition of different components on ECL signal with respect to a 10^{-6} M H_2O_2 addition in biosensor preparation: (a) immobilized $Ru(bpy)_3^{2+}$ in oxidized graphite; (b) chitosan membrane on immobilized $Ru(bpy)_3^{2+}$ in oxidized graphite; (c) uricase in chitosan membrane with immobilized $Ru(bpy)_3^{2+}$ in oxidized graphite SPE and (d) 10^{-4} M UA addition on $Ru(bpy)_3^{2+}$ immobilized in oxidized graphite SPE with uricase in chitosan membrane.

3.3.2. Enzyme and chitosan concentrations

The uricase in chitosan was immobilized over the graphite electrode containing $Ru(bpy)_3^{2+}$. Working with a constant and small amount of uricase (18.6 IU mL^{-1}), different concentrations of chitosan ranging from 0.5 g L^{-1} to 10 g L^{-1} were tested. The inhibition at a constant UA concentration, measured by v^0/v, increased with the chitosan concentration up to 2.5 g L^{-1} due to a better electrochemical environment. At higher concentrations of chitosan, the v^0/v was nearly constant although the membranes were brittle. For that reason, the last concentration was selected for biosensor preparation.

To optimize the enzyme concentration in the membrane, we measured membranes prepared with 5 μL of solutions containing from 18.6 to 185.6 IU mL^{-1} of the enzyme. The I^0/I value grows up to 93.0 IU mL^{-1}, and then stays constant. This concentration was used to prepare the biosensor.

3.4. Measurement conditions

Different studies were performed to optimize the experimental conditions for the use of the ECL biosensor, namely the voltage applied, waiting time, and pH.

3.4.1. pH dependence

The evolution of the S/N ratio with the pH shows two maxima at 7.9 (S/N ratio 18.9) and 9.0 (S/N 76.8) (Fig. 5B), as a result of two different pH influences: the ruthenium complex reduction and the enzymatic oxidation of UA. The use of a pH around 7.5 was indicated by Bard et al. [17] as the best condition for ECL reductive oxidation of the ruthenium complex. But we obtained the best S/N ratio at pH 9.0 due to the better enzymatic activity of the uricase [29] and this was used as the working pH.

ECL blank signal

$$O_2 + 2H^+ + 3e^- \xrightarrow{Uricase} OH^\bullet + OH^- \qquad E = -0.9\ V$$

$$Ru(bpy)_3^{2+} + e^- \rightarrow Ru(bpy)_3^{+} \qquad E = -1.1\ V$$

$$Ru(bpy)_3^{+} + OH^\bullet \rightarrow Ru(bpy)_3^{2+*} + OH^-$$

$$Ru(bpy)_3^{2+*} \rightarrow Ru(bpy)_3^{2+} + h\nu\ (620\ nm)$$

ECL co-reactant reaction:

$$UA + O_2 \xrightarrow{Uricase} H_2O_2 + allantoin$$

$$H_2O_2 + e^- \rightarrow OH^\bullet + OH^- \qquad E = -0.41\ V$$

$$Ru(bpy)_3^{2+} + e^- \rightarrow Ru(bpy)_3^{+} \qquad E = -1.1\ V$$

$$Ru(bpy)_3^{+} + OH^\bullet \rightarrow Ru(bpy)_3^{2+*} + OH^-$$

$$Ru(bpy)_3^{2+*} \rightarrow Ru(bpy)_3^{2+} + h\nu\ (620\ nm)$$

Co-reactant inhibition

$$OH^\bullet + UA \rightarrow OH^- + P1$$

$$Ru(bpy)_3^{+} + UA \rightarrow Ru(bpy)_3^{2+} + P2$$

Fig. 4. Uric acid biosensor mechanism. In this figure, P1 and P2 are unknown products of the reaction.

3.4.2. Selection of ECL potential

The influence of the applied potential on the ECL emission intensity was studied by cyclic voltammetry, between 1.7 V and −1.7 V. Two experiments were performed, the first measuring a solution of 10^{-6} M of H_2O_2 in the SPE cells without the enzymatic layer, and the second measuring a solution of uric acid in the SPE cells with the enzymatic layer (Fig. 5C). In both cases, the ECL signal increased up to −1.1 V and then decreased afterwards. The ECL did not appear at −1.3 V as Bard et al. indicates for $Ru(bpy)_3^{2+}$ in solution [17], due to the immobilization effect of the complex, which decreases the reduction potential to −1.1 V, improving the conductivity and making the reduction easier, obtaining a similar behavior to that reported by Premkumar et al. using graphite electrodes [22]. Additionally, the placement of an uricase membrane over the modified graphite does not affect the ECL potential.

3.4.3. Waiting time

In this case, the parameter used for waiting time optimization was the signal-to-noise ratio (S/N, where S is ν^0/ν) because the standard deviation decreases with time. A waiting time study from 0 to 5 min showed that the S/N ratio grew up to 3 min, then decreasing (Fig. 5D). Therefore, 3 min were selected.

3.5. Analytical characterization

3.5.1. Analytical signal

The analytical parameter used was neither the ECL intensity (I) after a short pulse (<5 s) nor the integration of the emission during a long time pulse (>1 min), because our enzymatic system generates growing ECL signals when successive pulses were applied. The use of the initial rate ($\nu = \Delta I/\Delta t$) estimated from several consecutive pulses regularly spaced, offers the best results in terms of accuracy. Thus, the analytical parameter in this case is the ratio of initial rate for blank and standard, respectively (ν^0/ν). Conditions as dwelling time and pulse time required to calculate the analytical parameter were optimized resulting 10 s and 1 s, respectively.

The quenching behavior observed for UA can be described using this analytical parameter by a Stern–Volmer type equation: $(\nu^0/\nu) = 1 + K_{SV_{app}}[UA]$ where ν^0 and ν represent the ECL initial rate estimations in the absence and presence of the quencher, and is the apparent Stern–Volmer constant that defines the efficiency of quenching [34].

Fig. 6 shows the profile of ECL when four pulses of −1.1 V were applied to five standards of uric acid ranging from 1.0×10^{-5} to 1.0×10^{-3} M and three replicates each. A linearized function was estimated using the above Stern–Volmer relationship, with an apparent Stern–Volmer constant of $1.84 \times 10^4\ M^{-1}$. The relative standard deviation calculated using different biosensors each time was 13.6% using 1×10^{-4} M UA ($n = 3$) and 14.6% ($n = 5$) for the blank (Table 1). The limit of detection (LOD) of the procedure using IUPAC standard criteria was 3.1×10^{-6} M. The analytical parameters are presented in Table 1.

A comparative study between different electrochemiluminescent uric acid biosensors from the bibliography [8,10] shows that these methods offered only one order of magnitude range (6×10^{-5} to 6×10^{-4} M) instead of the two orders obtained with our method. In the case of the limit of detection, the value that we found (3.1×10^{-6} M) is better than that obtained by Chen et al. (8.0×10^{-6} M). With respect to the reproducibility, the obtained values from the bibliography using conventional electrodes are better (around 3%) than our results (13.6%), due to the disposable

Table 1
Analytical parameters for UA SPE biosensor.

Parameter	Value	
Range, M	1.0×10^{-5} to 1.0×10^{-3}	
Ordinate	0.96 ± 0.08	
Slope	$18{,}430 \pm 1180$	
R^2	0.992	
LOD, M	3.1×10^{-6}	
LOQ, M	1.0×10^{-5}	
RSD (%) blank ($n = 5$)	14.6	
RSD (%) UA ($n = 3$)	1.0×10^{-4} M	13.6

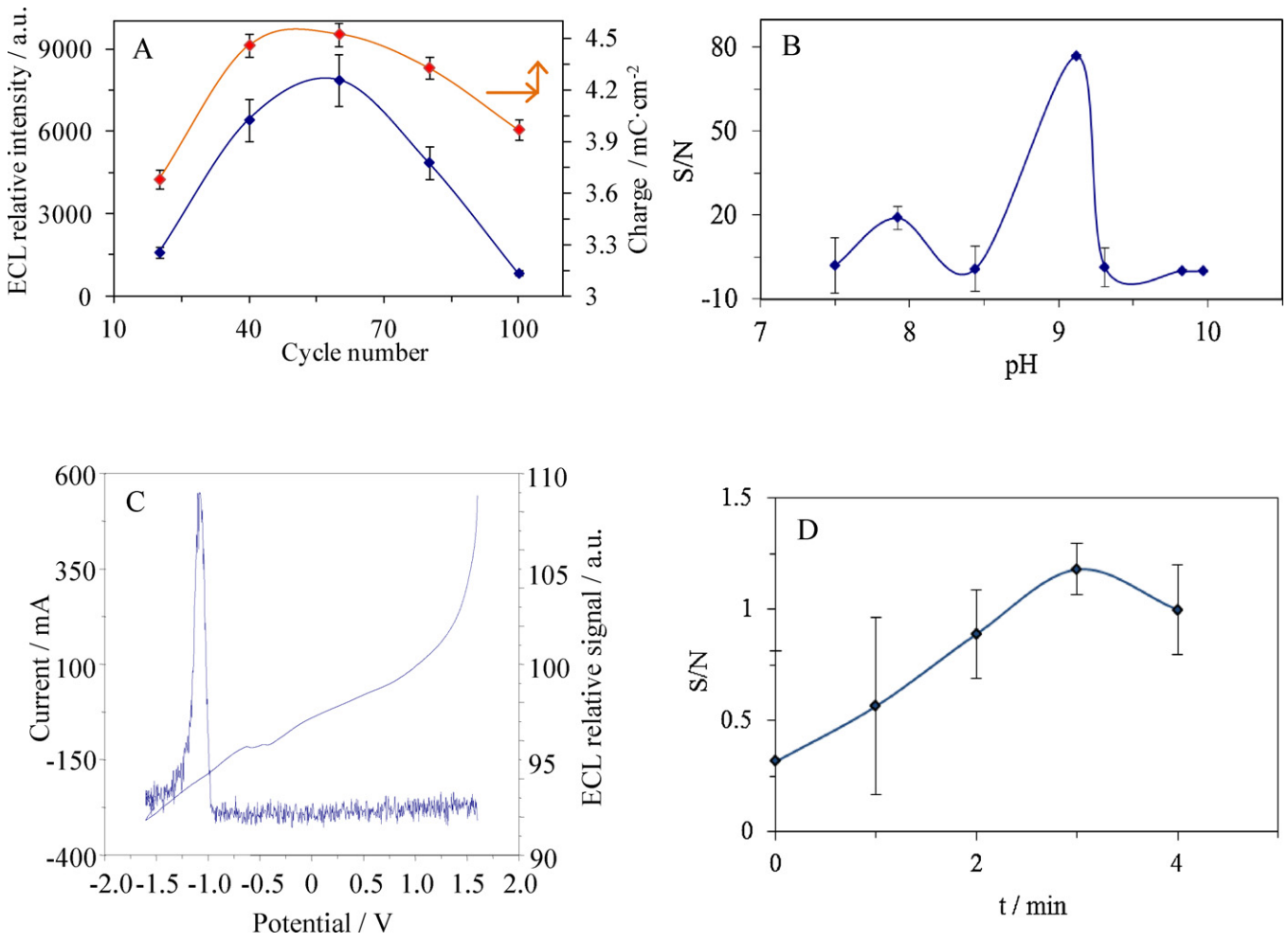

Fig. 5. Optimization parameters for the preparation of uric acid biosensor: (A) I^0/I ECL signals and net charge (upper line) for $Ru(bpy)_3^{2+}$ immobilization with respect to cycle number; (B) S/N ratio of the ECL signal with respect to pH; (C) study of the ECL emission using different voltages on an SPE cell with immobilized $Ru(bpy)_3^{2+}$ and 10^{-6} M H_2O_2 solution. Two reduction peaks are observed: one at −0.4 V, ascribed to H_2O_2, with no ECL outcome, and a second at −1.1 V, where ruthenium is reduced producing ECL emission; (D) waiting time after measurement for an optimum enzyme conversion.

format used. Comparing the results with those of an ECL biosensor based on luminol and uricase previously developed by us [6], we note that this has a lower limit of detection (4.4×10^{-7} M) and similar precision (9.3%).

We conclude that using an inhibition method makes it possible to obtain similar results to those obtained with conventional ECL methodology.

3.6. Interference study

Of the different species present in the urine samples such as K^+, NH_4^+, Mg^{2+}, glucose, lactose, urea and ascorbic acid, only two of them, urea or ascorbic acid, acts as interferences.

According to Burtis and Ashwood [35], the normal levels of urea are 428–714 mmol/24 h. To study the influence of urea, we tested

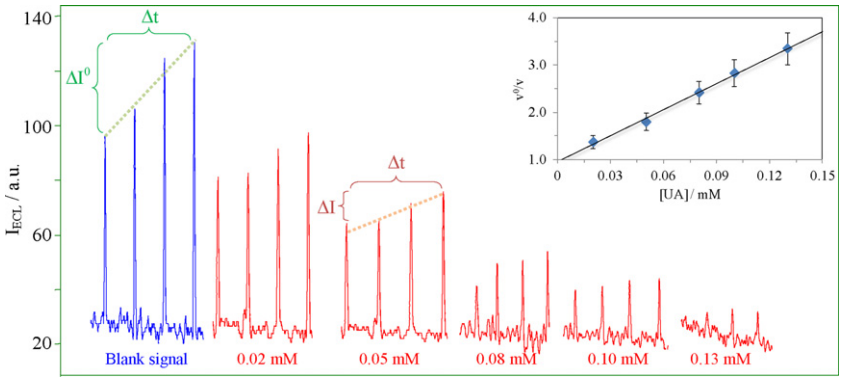

Fig. 6. Illustration of ECL experimental data from uric acid standards at different concentrations. This shows: (1) an ECL intensity decay when uric acid concentrations are increased and (2) a progressive ECL intensity growth when different pulses are applied to the SPE cells due to enzymatic production of H_2O_2. Observe that the initial rate estimation obtained from the slope of the different standards (the analytical signal) decreases with an increase of UA concentration. The inset shows the obtained Stern–Volmer calibration.

Table 2
Determination of UA in urine samples by proposed and reference procedures.

Urine samples	ECL biosensor, M	Reference procedure, M	*p*-Value, %	%
1	$(1.32 \pm 0.14) \times 10^{-3}$	$(1.35 \pm 0.01) \times 10^{-3}$	74.2	97.5
2	$(2.66 \pm 0.36) \times 10^{-3}$	$(2.50 \pm 0.01) \times 10^{-3}$	49.6	106.4
3	$(3.13 \pm 0.25) \times 10^{-3}$	$(3.10 \pm 0.10) \times 10^{-3}$	84.2	101.1

concentrations between 0.2 and 0.8 mM in order to maintain the same UA/urea ratio (real ratio 0.428 and 0.71 mM) working at a level of 0.05 mM in UA. The results show a small decrease in the signal (0.47 times) from 0.4 mM (tolerance limit).

In the case of ascorbic acid, the normal level is 0.30–0.36 mmol/24 h and using the same considerations as above (0.05 mM in UA), the studied concentration should be between 0.0030 mM and 0.0036 mM, but as the interference level in this range is very low, we studied the influence between 0.01 and 1 mM. In this case, an increase in the ECL signal was observed, with a tolerance limit of 0.2 mM, increasing the signal 2.93 times.

Ascorbic acid acts as a co-reactant in ECL with ruthenium at positive potentials [36]. However, the reduction potential of ascorbic acid in alkaline conditions takes values around −0.06 V [37]. It is possible that a reductive oxidation mechanism occurs, increasing the ECL emission, which is a positive interference in this system.

3.7. Application to urine samples

The biosensor was applied for uric acid determination in urine samples. A 24 h-urine sample was taken and diluted 100-fold with a 0.2 M phosphate buffer at pH 9.0 with 0.25 M of NaCl. Working with this dilution, a constant and low interference was obtained from the urine matrix that was eliminated by a blank correction with no need for sample filtration or a standard addition calibration for every sample. The validation was performed by comparing the results obtained using the biosensor and a conventional clinical auto-analyzer method. The obtained statistics results, in *p*-values, were higher than 5% (Table 2).

4. Conclusions

An ECL biosensor in disposable format prepared on graphite screen-printed cells for uric acid analysis in urine is presented. The reagents needed for the ECL production are immobilized on the working electrode. The transduction chemistry is based on an electrochemically immobilized $Ru(bpy)_3^{2+}$ complex forming a composite in the graphite working electrode. The recognition chemistry is placed as a chitosan upper layer containing uricase. The uric acid biosensing is based on an ECL inhibition behavior between the co-reactants and more precisely on the quenching produced by uric acid over the cathodic ECL caused by immobilized $Ru(bpy)_3^{2+}$ in the presence of uricase. A possible ECL mechanism based on the consumption of co-reactant intermediates with no ECL emission is proposed. To the best of our knowledge, this is the first ECL biosensor for uric acid based on the enzymatic production of H_2O_2 using $Ru(bpy)_3^{2+}$ as luminophore. The cathodic ECL quenching effect of uric acid produces a new biosensor in a disposable format for the analysis of uric acid in urine.

Acknowledgements

We acknowledge financial support from the Ministerio de Ciencia e Innovación, Dirección General de Investigación y Gestión del Plan Nacional de I+D+i (Spain) (Projects CTQ2009-14428-C02-01 and CTQ2009-14428-C02-02); and the Junta de Andalucía (Proyecto de Excelencia P08-FQM-3535). These projects were partially supported by European Regional Development Funds (ERDF). We acknowledge Francisco Montilla, associate professor at the University of Alicante, Alicia Aldaya from Ruiz de Alda Granada Hospital, and PhD student Javier Ametis for his helpful and kind assistance.

References

[1] H. Kaur, B. Halliwell, Chem.-Biol. Interact. 73 (1990) 235–247.
[2] U.M. Khosla, S. Zharikov, J.L. Finch, T. Nakagawa, C. Roncal, W. Mu, K. Krotova, E.R. Block, S. Prabhakar, R.J. Johnson, Kidney Int. 67 (2005) 1739–1742.
[3] D.L. Kasper, T.R. Harrison, Harrison's Principles of Internal Medicine, 16th ed., McGraw-Hill, Medical Pub. Division, New York, 2005.
[4] T. Ahuja, Rajesh, D. Kumar, V.K. Tanwar, V. Sharma, N. Singh, A.M. Biradar, Thin Solid Films 519 (2010) 1128–1134.
[5] J. Arora, S. Nandwani, M. Bhambi, C.S. Pundir, Anal. Chim. Acta 647 (2009) 195–201.
[6] J. Ballesta-Claver, I.F. Díaz Ortega, M.C. Valencia-Miron, L.F. Capitán-Vallvey, Anal. Chim. Acta 702 (2011) 254–261.
[7] C.A. Marquette, L.J. Blum, Sens. Actuators B 90 (2003) 112–117.
[8] Z. Lin, Z. Chen, Y. Liu, J. Wang, G. Chen, Analyst 133 (2008) 797–801.
[9] Y. Chi, Y. Dong, G. Chen, Anal. Chem. 79 (2007) 4521–4528.
[10] Z. Chen, Y. Zu, J. Electroanal. Chem. 612 (2008) 151–155.
[11] H. Wei, E. Wang, TrAC: Trends Anal. Chem. 27 (2008) 447–459.
[12] R. Ye, L. Huang, B. Qiu, Z. Song, Z. Lin, G. Chen, Luminescence 26 (2011) 531–535.
[13] Z. Lin, J. Sun, J. Chen, L. Guo, G. Chen, Electrochim. Acta 53 (2007) 1708–1712.
[14] Y.D. Liang, C.X. Yu, J.F. Song, Luminescence 26 (2011) 662–669.
[15] X. Lu, D. Liu, J. Du, H. Wang, Z. Xue, X. Liu, X. Zhou, Analyst 137 (2012) 588–594.
[16] K.A. Fahnrich, M. Pravda, G.G. Guilbault, Talanta 54 (2001) 531–559.
[17] J.P. Choi, A.J. Bard, Anal. Chim. Acta 541 (2005) 141–148.
[18] M.A. Carvajal, J. Ballesta-Claver, D.P. Morales, A.J. Palma, M.C. Valencia-Mirón, L.F. Capitán-Vallvey, Sens. Actuators B 169 (2012) 46–53.
[19] L.A. Kaplan, A.J. Pesce, Clinical Chemistry Theory, Analysis and Correlation, St. Louis, Mosby, 1984.
[20] J. Ballesta-Claver, M.C. Valencia-Miron, L.F. Capitán-Vallvey, Analyst 134 (2009) 1423–1432.
[21] L. Guo, L. Xue, B. Qiu, Z. Lin, D. Kim, G. Chen, Phys. Chem. Chem. Phys. 12 (2010) 12826–12832.
[22] J. Premkumar, S.B. Khoo, Electrochem. Commun. 6 (2004) 984–989.
[23] H.P. Dai, K.K. Shiu, J. Electroanal. Chem. 419 (1996) 7–14.
[24] P.K. Mallick, G.D. Danzer, D.P. Strommen, J.R. Kincaid, J. Phys. Chem. 92 (1988) 5628–5634.
[25] M. Xiang, R. Lei, N. Li, K. Li, J. Appl. Electrochem. 39 (2009) 921–925.
[26] C. Zhao, L. Wan, Q. Wang, S. Liu, K. Jiao, Anal. Sci. 25 (2009) 1013–1017.
[27] H. Dai, X. Wu, H. Xu, Y. Wang, Y. Chi, G. Chen, Electrochim. Acta 54 (2009) 4582–4586.
[28] H. Cui, X.Y. Zhao, X.Q. Lin, Luminescence 18 (2003) 199–202.
[29] G.P.A. Bongaerts, J. Uitzetter, R. Brouns, G.D. Vogels, Biochim. Biophys. Acta: Enzymol. 527 (1978) 348–358.
[30] O.M. Pitts, D.G. Priest, W.W. Fish, Biochemistry 13 (2002) 888–892.
[31] S. Qiu, S. Gao, X. Zhu, Z. Lin, B. Qiu, G. Chen, Analyst 136 (2011) 1580–1585.
[32] R. Radi, H. Rubbo, L. Thomson, E. Prodanov, Free Radic. Biol. Med. 8 (1990) 121–126.
[33] A. Sassolas, L.J. Blum, B.D. Leca-Bouvier, Anal. Bioanal. Chem. 394 (2009) 971–980.
[34] J.R. Lakowicz, Principles of Fluorescence Spectroscopy, 3rd ed., Springer, Heidelberg, 2006.
[35] C.A. Burtis, E.R. Ashwood, Tietz Fundamentals of Clinical Chemistry, 3rd ed., Saunders, Philadelphia, 1999.
[36] F. Takahashi, J. Jin, Luminescence 23 (2008) 121–125.
[37] J.C. Ghosh, T.L.R. Char, Z. Physiol. Chem. 246 (1937) 115–123.